Methods xxx (2010) xxx–xxx

Contents lists available at ScienceDirect

Methods

journal homepage: www.elsevier.com/locate/ymeth

Spatial expression profiles in the *Xenopus laevis* oocytes measured with qPCR tomography

Radek Sindelka [a], Monika Sidova [b,c], David Svec [b], Mikael Kubista [b,d,*]

[a] *Whitehead Institute, Cambridge, USA*
[b] *Laboratory of Gene Expression, Institute of Biotechnology, Academy of Sciences of the Czech Republic, Prague, Czech Republic*
[c] *Charles University in Prague, Faculty of Science, Department of Cell Biology, Czech Republic*
[d] *TATAA Biocenter AB, Odinsgatan 28, 411 03 Göteborg, Sweden*

ARTICLE INFO

Article history:
Accepted 18 December 2009
Available online xxxx

Keywords:
Xenopus
Oocyte
qPCR tomography
Expression profiling

ABSTRACT

qPCR tomography was developed to study mRNA localization in complex biological samples that are embedded and cryo-sectioned. After total RNA extraction and reverse transcription, the spatial profiles of mRNAs and other functional RNAs were determined by qPCR. The *Xenopus laevis* oocyte was selected as model, because of its large size (more than 1 mm) and large amount of total RNA (~5 μg). Fifteen sections along the animal–vegetal axis were cut and prepared for quantification of 31 RNA targets using the high-throughput real-time RT-PCR (qPCR) BioMark™ platform. mRNAs were found to have two localization patterns, animal/central or vegetal. Because of the high resolution in sectioning, it was possible to distinguish two subgroups of the vegetal gene patterns: germ plasm determinant pattern and profile of other vegetal genes.

1. Introduction

The early development of a multicellular organism is a complex process in which each step must be precisely controlled. Each cell has unique expression of genes and the spatial gene expression patterns within the growing embryo depend on the cells' position.

In situ hybridization, microarray analyses, RNA protection assays, RT-PCR, Illumina sequencing and real-time quantitative PCR (qPCR) are among the most frequently used methods for gene expression analysis. Each method has its limitations and comparison of results between laboratories using different methods including different conditions and protocols is difficult. For example, while whole mount *in situ* hybridization is standard for spatial analysis in developmental biology, quantification of gene expression is at best qualitative. On the other hand, high-throughput quantitative methods such as microarrays and Illumina sequencing can produce large amounts of quantitative expression data. However, spatial resolution is limited using these methods since they require large amounts of pure and high quality RNA. qPCR is in-between; quantification is highly precise and minute amounts of RNA can be used, which allows for spatial profiling. Tens of genes can be conveniently quantified in each sample.

Oogenesis in *Xenopus laevis* results in oocytes with 1.3 mm in diameter [1]. Mature oocytes have differently colored hemispheres that specify the developmental animal–vegetal axis. Pigmentation of the animal hemisphere is caused by accumulation of melanosomes. The animal hemisphere also contains the germinal vesicle. The light color of the vegetal hemisphere is due to storage of yolk platelets [2].

mRNA molecules synthesized during oogenesis are termed maternal, because the template for their transcription is solely maternal chromosomes (reviewed in [3]). Two groups of maternal transcripts have been identified that differ in their spatial distribution in the *Xenopus* oocyte (reviewed in [4–6]). One group is called vegetal. These genes are expressed during the early stages of oogenesis and the corresponding mRNA molecules are actively transported from the nucleus to the vegetal pole. Two different transport pathways have been identified. DEADSouth, Xcad2, Xdazl and Xpat transcripts are transported by the early METRO (message transport organizer) pathway [7,8] and they accumulate in the primordial germ cells formed in later developmental stages. The second pathway is active later during oogenesis and transports mRNA molecules, such as VegT and Vg1, that are important for germ layer determination. The vegetal hemisphere gives rise to the endoderm cell layer in later stages of development and stimulates the formation of the mesodermal layer. mRNAs encoded by many maternal genes including An1, An2, An3, Tcf-1, axin, Xpar1 localize predominantly in the animal hemisphere [4–6,9].

The distribution of mRNAs along the animal–vegetal axis in the *Xenopus* oocyte is critical for successful development. The second

* Corresponding author. Address: Laboratory of Gene Expression, Institute of Biotechnology, Academy of Sciences of the Czech Republic, Prague, Czech Republic. Fax: +46 31 152890.
E-mail address: mikael.kubista@tataa.com (M. Kubista).

1046-2023/$ - see front matter © 2010 Elsevier Inc. All rights reserved.
doi:10.1016/j.ymeth.2009.12.011

developmental axis, the dorsal–ventral, can be distinguished at the 4-cell stage in *Xenopus*. The sperm enters the oocyte at a random position in the animal pole. This is followed by the cortical rotation approximately 20 min after the fertilization [10–12], during which the vegetal cortex layer moves approximately 30° in the opposite direction to the sperm's entry. This results in the accumulation of beta-catenin and some yet unknown stabilizing factors into the forthcoming dorsal side of the embryo. Surprisingly, the cortical rotation does not significantly change the distribution of maternal mRNAs along the A–V axis [9].

In this paper we present the high resolution qPCR tomography technique for spatiotemporal analysis of mRNAs in the *X. laevis* oocyte. We present the entire procedure from sample preparation, embedding, slicing, RNA extraction, reverse transcription, preamplification, qPCR to data analysis. In our study, *X. laevis* oocytes were sectioned into 15 segments across the animal–vegetal (A–V) axis and the levels of 31 maternal transcripts, mitochondrial RNAs, and nucleus specific RNAs were quantified using the high-throughput real-time RT-PCR microfluidic BioMark™ platform (www.fluidigm.com).

2. Materials and methods

2.1. Embryo fixation and sectioning

Xenopus laevis females were stimulated with 500 U of hCG (human chorionic gonadotrophin) and kept overnight in room temperature. Oocytes were obtained by gentle squeezing. They were not treated with cysteine, which is common procedure, because the treatment compromises the subsequent cryo sectioning of the samples. Three oocytes from the same female were used in our study. The oocytes were embedded in a drop of optimum cutting temperature (OCT) on a pre-cooled dissection block (Microm HM560). The block was placed for 5 min at −20 °C in the cryostat chamber and the samples were dissected into 45 slices each 30 μm thick along the animal–vegetal (A–V) axis (Fig. 1). Consecutive slices were pooled into fifteen tubes with three slices in each. Hence, the first tube contained the first three animal sections, the second tube contained sections 4–6, etc., and tube fifteen contained the last three vegetal sections.

2.2. Extraction of total RNA and quality control

The RNeasy Micro kit (Qiagen) was used for total RNA extraction. RLT (350 μl) RNeasy lysis buffer with 1% mercaptoethanol and RNA carrier was added to each tube, which were immediately stored at −80 °C. After thawing of the samples they were vortexed for at least 1 min in lysis buffer. The mercaptoethanol added and the long vortexing were found to be essential for efficient removal of inhibitors. Yolk platelets localized in the vegetal part of the oocyte were found serious inhibitor of reverse transcription and qPCR. RNA concentrations were measured with the Nanodrop® ND1000 quantification system (Nanodrop Inc., Fig. 1).

Quality of the extracted RNA was assessed by running 10 randomly selected samples on the capillary electrophoresis system Experion (Bio-Rad). Total RNA (50 ng) was denatured and loaded into the HighSense chip and run according to the manufacturer's protocol (Fig. 2). An 18S to 28S ribosomal RNA ratio of 1:2 indicated high quality RNA. High quality RNA is further supported by the absence of short RNA fragments that would indicate degradation.

2.3. Reverse transcription

cDNA was produced starting with 30 ng of total RNA, 1.5 μl of a (1:1) mixture of 10 μM oligo-dT and 10 μM random hexamers and water. Total reaction volume was 8.5 μl. After 10 min incubation at 72 °C, 100 U of MMLV reverse transcriptase (Promega), 12 U of RNasin (Promega), 5 nmol of dNTP and 2 μl of buffer (5×) were added to a total volume of 11.8 μl. The mixture was incubated for 60 min at 37 °C. The cDNA product was diluted to 60 μl and stored at −20 °C.

2.4. Primer design and preamplification

Primers for the amplification of the 31 selected maternal genes were designed with Primer3 [http://frodo.wi.mit.edu/primer3/]. Primer specificity and assay efficiency was tested on control cDNA (mixture of cDNA from different *Xenopus* developmental stages). Acceptance criteria were: specific amplification of control cDNA with a Cq lower than 35, a single dominant peak in the derivative of the melting curve, and no amplification of non-template controls.

Preamplification was used to increase the number of template molecules. This is needed because the cDNA synthesis does not yield sufficient number of molecular copies of the template molecules that they can be analyzed with confidence in parallel singleplex reactions. Preamplification PCR was run in 20 μl containing 4 μl of cDNA, 2 μl of a mixture of all forward and reverse primers (500 nM each), 10 μl of Sigma JumpStart mastermix (Sigma, cus-

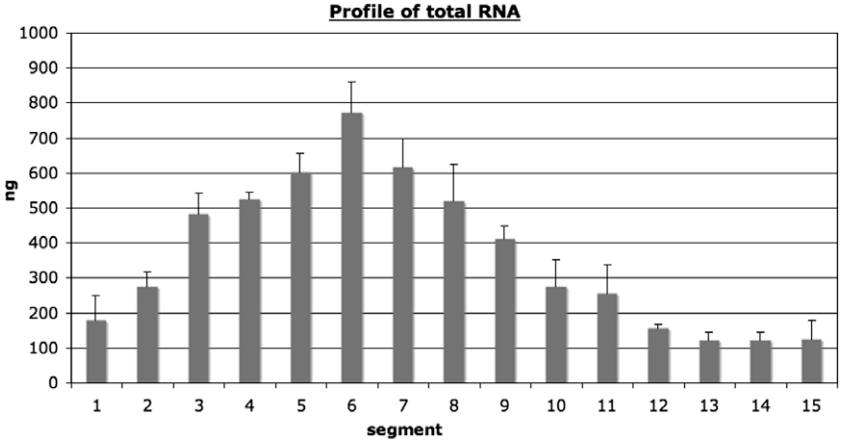

Fig. 1. Spatial distribution of total RNA in the *Xenopus laevis* oocyte. Oocytes were sectioned across the A–V axis. Total RNA was extracted and quantified using the Nanodrop. Each bar represents a 90 μm section.

Please cite this article in press as: R. Sindelka et al., Methods (2010), doi:10.1016/j.ymeth.2009.12.011

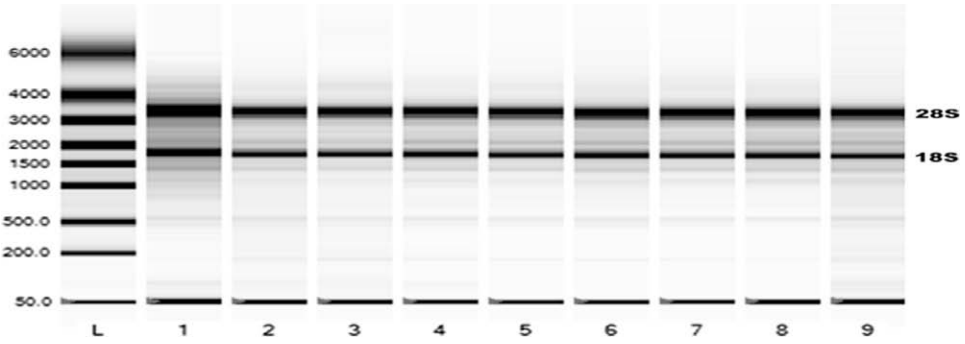

Fig. 2. The quality of the extracted RNA was assessed with capillary electrophoresis (Experion, Bio-Rad). Total RNA (100 ng) from 11 sections were analyzed on high sense chip.

tomized product) and water. A CFX 96 cycler (Bio-Rad) was used for the preamplification with the cycling conditions: polymerase activation at 95 °C for 2 min, followed by 18 cycles (95 °C 15 s, 59 °C 1 min and 72 °C 1 min). The product of the preamplification reaction was diluted to 80 µl and stored at −20 °C. The robustness of the preamplification was validated by comparing qPCR expression levels of the genes Xmam1 and Vg1 that were analyzed with and without preamplification. The relative expression of the two genes was similar when analyzing data with and without preamplification (Fig. 3).

2.5. High-throughput qPCR performed on Biomark system

The high throughput microfluidic qPCR platform BioMark™ (Fluidigm) was used for qPCR analysis running the 48.48 dynamic array. The sample reaction mixtures had a final volume of 5.3 µl made up of 1.2 µl preamplified cDNA, 0.6 µl of SYBR Green Sample Loading reagent (Fluidigm), 2.77 µl Sigma A mastermix (Sigma, custom product), 0.165 µl of Chromophy, diluted 1:25 (TATAA Biocenter), 0.025 µl of ROX (Invitrogen) and 0.1 µl of JumpStart DNA Taq polymerase (Sigma). The primer reaction mixtures had also a final volume of 6 µl and were made up of 3 µl Assay Loading reagent (Fluidigm) and 3 µl of a mixture of reverse and forward primers (10 µM). The empty dynamic array was first primed with oil solution in the NanoFlex™ 4-IFC Controller (Fluidigm) to fill its control valves. Sample reaction mixtures were loaded into the sample wells carefully avoiding any bubbles, and primer reaction mixtures were loaded into the assay wells. The dynamic array was then placed again into the NanoFlex™ 4-IFC Controller for loading and mixing. The mixing takes place by diffusion between the reaction chambers filled with sample reagent and adjacent containers filled with the appropriate primer and probe mix, between which a channel is opened. After about 55 min the dynamic array was transferred to the BioMark™. The qPCR cycling program was 3 min at 95 °C for activation of the hot-start enzyme, followed by 30 cycles of denaturation at 95 °C for 15 s, annealing at 60 °C for 20 s, and elongation at 72 °C for 20 s. Melting curves analysis was performed after completed qPCR collecting fluorescence between 60 and 95 °C at 0.5 °C increments.

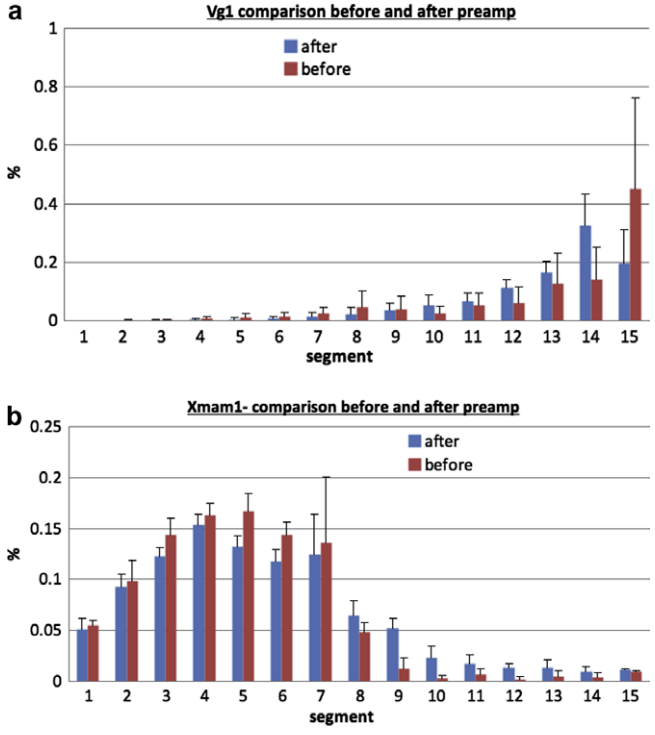

Fig. 3. Comparison of the spatial expression profiles of Vg1 (vegetal gene) and Xmam1 (animal genes) measured with and without preamplification.

2.6. Data analysis

Specific amplification of each targeted cDNA was confirmed by melt curve analysis. Measured Cq values were exported from the BioMark™ platform software to Excel for data analysis. qPCR technical replicates of samples were averaged. Expression ratios were calculated by the delta Cq method normalized to the first animal tube (containing sections 1–3). This artificially sets the expression of all genes in the first segment to 1, relative to which all other segments are expressed. For each oocyte and separately for every gene the relative expressions in all segments were summed, and the data were divided with the sum. This resulted in expression of each gene being presented as the percentage of its total expression. The percentage values for the three oocytes were finally averaged. The averaged values and associated standard deviations are presented. The standard deviations were in general very small and cannot be seen in the plot.

3. Results

During optimization of sample collection and preparation for cryosectioning we found that extensive cysteine treatment, which is common in many protocols, makes oocytes fragile and lowers the quality of the RNA. Because of the large size (1.3 mm in diameter) of the *X. laevis* oocyte, different thickness of the cryostat sections is possible. We found that 30 µm sections, which is the maximum width possible with our cryostat (Microm), worked very well and most oocytes gave the same number of sections. We also

found that pre-incubation of the samples in the cryostat chamber for at least 10 min was important for smooth sectioning. Mercaptoethanol (1%) was critical not only for reducing the activity of RNases, but also for removal of the yolk and other lipids from the vegetal pole. Once the protocol was optimized, the variability in total RNA concentration between segments cut from different oocytes was very low, evidencing precise and reproducible sectioning and RNA extraction (Fig. 1). The quality of the extracted RNA was assessed with capillary electrophoresis using the Experion system (Bio-Rad), and indicated high quality RNA (Fig. 2).

The reaction chambers in the BioMark™ platform are only 10 nl and the loaded cDNA is automatically aliquoted into 48 chambers. For each chamber to contain sufficient cDNA for reliable quantification the material must be preamplified. The performance of the preamplification was tested by comparing one vegetal gene (Vg1) and one animal gene (Xmam1) with and without preamplification. The relative expression of the two genes was the same suggesting that preamplification introduces minimal bias (Fig. 3).

Two main spatial expression profiles were found for the 31 maternal genes studied. Most were abundant in the upper third of the oocyte, which is in the animal hemisphere probably close to the oocyte nucleus. Genes frequently used for normalization of expression in *X. laevis* [13], such as EF-1alpha, GAPDH, beta-tubulin, alpha-actin and RNA polymerase II had this localization. Mitochondrial cytochrome C mRNAs and U3 snoRNA, which is located in the nucleolus, were also localized to the animal hemisphere (Figs. 4 and 5). The high resolution of qPCR tomography allowed two subgroups within the vegetal genes to be distinguished (Fig. 6). The spatial distribution of germ plasm determinants such as Xdazl, DEADSouth and Xcad2 shows a very steep gradient toward the vegetal pole, suggesting that these mRNAs are localized densely close to the pole itself [14]. Vg1, VegT, Otx1, Eg6 and Wnt11 are also localized vegetal, but with a less steep spatial gradient toward the pole.

4. Conclusions

qPCR tomography was introduced by Sindelka et al., in 2008. In the pioneer work *X. laevis* oocytes were sectioned into five segments across the animal–vegetal axis and expression levels of 18 maternal genes were measured by qPCR. Two distinct expression patterns were found that were referred to as animal and vegetal. In the presented study, we refine the qPCR tomography technique to increase its resolution to 15 segments. This allowed us to distinguish two subgroups of the vegetal genes.

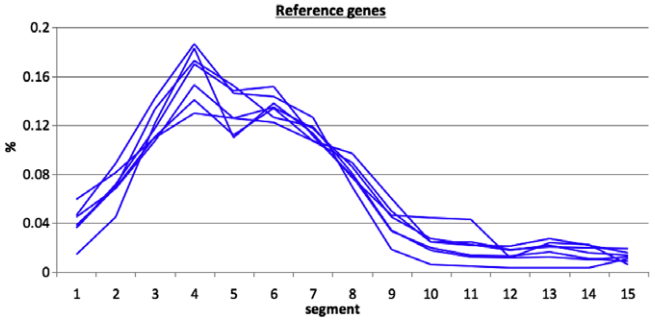

Fig. 4. Spatial expression profiles of common reference genes, mitochondrial RNA, reflecting the distribution of mitochondria in the cell, and nucleolar RNA, reflecting the position of the nucleus, along the A–V axis of the *X. laevis* oocyte. Distributions of mRNA coding RNA polymerase 2, mitochondrial cytochrome C, GAPDH, EF-1alpha, beta-tubulin, alpha-actin and U3 snoRNA was determined in 15 serial segments.

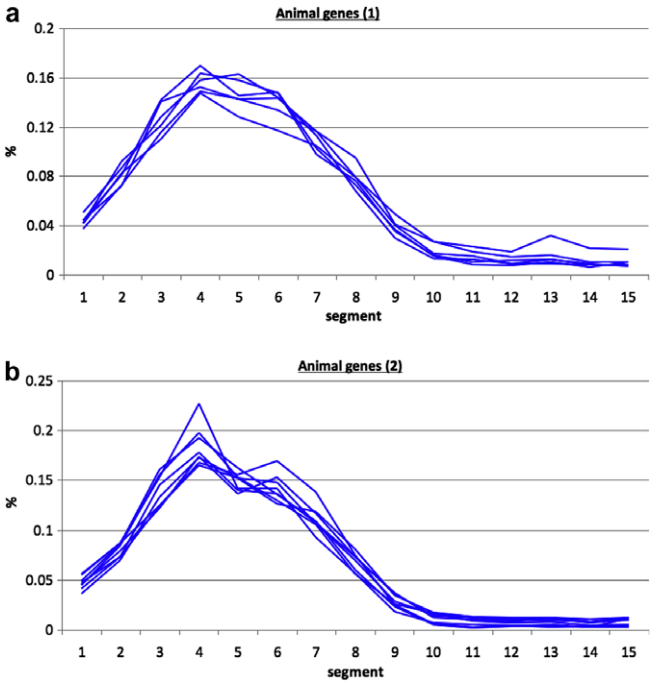

Fig. 5. Expression profiles of animal genes along the A–V axis of *X. laevis* oocyte. The distribution of mRNAs coding for An1, An2, APC, axin, Est1, Fz7, Zp3 and ZPC (1) and Xmam1, XPar1, Tcf-3, Stat3, Oct60, GSK-3beta and FoxH1 (2) was determined in 15 serial segments.

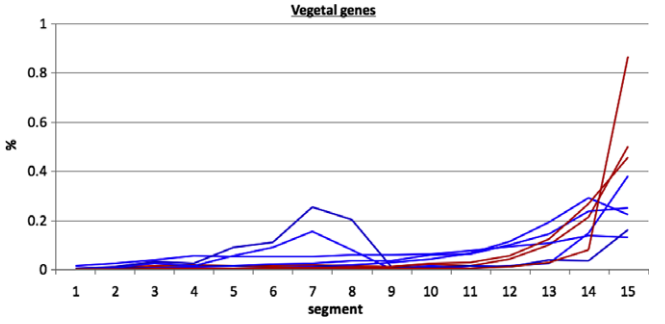

Fig. 6. Expression profiles of vegetal genes along the A–V axis of the *X. laevis* oocyte. The distribution of mRNA coding germ plasm factors Deadsouth, Xdazl and Xcad2 (in red) and other vegetal genes Otx1, Eg6, Vg1, VegT and Wnt11 (in blue) was determined in 15 serial segments.

The majority of mRNA molecules encoded by animal genes were found in sections 3–8. This is where the oocyte nucleus is expected to be located. This may indicate that animal transcripts are localized in the nucleus or stored somewhere near it. Interestingly, common reference genes used in *Xenopus* expression studies, such as EF-1alpha, GAPDH, beta-tubulin and alpha-actin, have animal localization. Clearly, they would not be suitable for normalization of spatial expression in the *Xenopus* oocyte and not even in early blastomere stages, where the original spatial distribution remains (unpublished data).

The higher sensitivity, better specificity and wider dynamic range of qPCR tomography compared to other RNA based methods allow spatial expression profiles to be measured with higher resolution than has been possible. Previous studies on single cell expression profiling have indicated large variations in the mRNA levels among cells [15,16]. This does not seem to apply to the *Xenopus* oocyte. The intracellular expression profiles seem to be highly conserved among the oocytes, indicating that mRNA spatial distribution is critical for the early development.

Please cite this article in press as: R. Sindelka et al., Methods (2010), doi:10.1016/j.ymeth.2009.12.011

Acknowledgments

This work was supported by Grant agency of Academy of Science Czech Republic (IAA500970904) and research goal AV0Z50520701 granted by Ministry of Youth, Education and Sports of the Czech republic, together with support from Grant agency of Czech Republic (GACR 301/09/1752).

References

[1] P. Chang, D. Perez-Mongiovi, E. Houliston, Microsc. Res. Tech. 44 (1999) 415–429.
[2] M.V. Danilchik, J.C. Gerhart, Dev. Biol. 122 (1987) 101–112.
[3] J. Heasman, Semin. Cell Dev. Biol. 17 (2006) 93–98.
[4] M.L. King, T.J. Messitt, K.L. Mowry, Biol. Cell 97 (2005) 19–33.
[5] Y. Zhou, M.L. King, IUBMB Life 56 (2004) 19–27.
[6] K.L. Mowry, C.A. Cote, FASEB J. 13 (1999) 435–445.
[7] H. MacArthur, M. Bubunenko, D.W. Houston, M.L. King, Mech. Dev. 84 (1999) 75–88.
[8] H. MacArthur, D.W. Houston, M. Bubunenko, L. Mosquera, M.L. King, Mech. Dev. 95 (2000) 291–295.
[9] R. Sindelka, J. Jonak, R. Hands, S.A. Bustin, M. Kubista, Nucleic Acids Res. 36 (2) (2008) 387–392.
[10] J. Gerhart, M. Danilchik, T. Doniach, S. Roberts, B. Rowning, R. Stewart, Development 107 (1989) 37–51.
[11] J.C. Gerhart, J.P. Vincent, S.R. Scharf, S.D. Black, R.L. Gimlich, M. Danilchik, Philos. Trans. R. Soc. Lond. B Biol. Sci. 307 (1984) 319–330.
[12] J.P. Vincent, J.C. Gerhart, Dev. Biol. 123 (1987) 526–539.
[13] R. Sindelka, Z. Ferjentsik, J. Jonak, Dev. Dyn. 235 (2006) 754–758.
[14] F. Nishiumi, T. Komiya, K. Ikenishi, Dev. Growth Differ. 47 (1) (2005) 37–48.
[15] M. Bengtsson, A. Stahlberg, P. Rorsman, M. Kubista, Genome Res. 15 (2005) 1388–1392.
[16] A. Tichopad, R. Kitchen, I. Riedmaier, C. Becker, A. Ståhlberg, M. Kubista, Clin. Chem. 55 (10) (2009) 1816–1823.